

Received: 2019.06.28
Accepted: 2019.10.11
Published: 2020.01.31

Upregulation of the Coatomer Protein Complex Subunit beta 2 (COPB2) Gene Targets microRNA-335-3p in NCI-H1975 Lung Adenocarcinoma Cells to Promote Cell Proliferation and Migration

Authors' Contribution:
Study Design A
Data Collection B
Statistical Analysis C
Data Interpretation D
Manuscript Preparation E
Literature Search F
Funds Collection G

ADE 1,2 **Xiaolin Pu**
BF 2 **Hua Jiang**
BD 1 **Wei Li**
EF 3 **Lin Xu**
CD 4 **Lin Wang**
CE 1 **Yongqian Shu**

1 Department of Oncology, The First Affiliated Hospital of Nanjing Medical University, Nanjing, Jiangsu, P.R. China
2 Department of Oncology, The Affiliated Changzhou No. 2 People's Hospital with Nanjing Medical University, Nanjing, Jiangsu, P.R. China
3 Department of Thoracic Surgery, Jiangsu Cancer Hospital, Nanjing, Jiangsu, P.R. China
4 Department of Oncology, Jiangsu Province Geriatric Institute, Nanjing, Jiangsu, P.R. China

Corresponding Author: Yongqian Shu, e-mail: yoqs_shuq@163.com
Source of support: Departmental sources

Background: The coatomer protein complex subunit beta 2 (COPB2) gene is upregulated and promotes cell proliferation in some cancer cells. This study aimed to investigate the role of microRNA (miRNA) targeting by COPB2 gene expression in human lung adenocarcinoma cell lines, including NCI-H1975 cells.


Material/Methods: COPB2 expression in normal human bronchial epithelial cells and lung adenocarcinoma cells was measured by quantitative reverse transcription-polymerase chain reaction (qRT-PCR) and Western blot. NCI-H1975 human lung adenocarcinoma cells were transfected with short-interfering COPB2 (siCOPB2). Cell apoptosis and cell proliferation were evaluated by flow cytometry and Cell Counting Kit-8 (CCK-8) assays, respectively. The transwell assay evaluated cell migration. Targeting of miR-335-3p by COPB2 was predicted using TargetScan 7.2 and verified using a dual-luciferase reporter assay in NCI-H1975 cells. MiR-335-3p mimics were transfected into NCI-H1975 cells. The further functional analysis included detection of protein expression for cyclin D1, tissue inhibitor matrix metalloproteinase-1 (TIMP-1), matrix metalloproteinase 9 (MMP9), Bcl-2, and Bax, to verify the role of miR-335-3p targeting by COPB2 in lung adenocarcinoma cells.

Results: COPB2 was upregulated in lung adenocarcinoma cells and was a direct target of miR-335-3p mimics. COPB2 knockdown promoted cell apoptosis, inhibited cell migration and proliferation in NCI-H1975 cells. The effects of COPB2 knockdown on NCI-H1975 cells were increased by miR-335-3p mimics, which also further reduced the expression levels of cyclin D1, MMP9, and Bcl-2 and further increased TIMP-1 and Bax by siCOPB2.

Conclusions: This study showed that COPB2 was the functional target of miR-335-3p in NCI-H1975 human adenocarcinoma cells.

MeSH Keywords: **Adenocarcinoma • Coatomer Protein • MicroRNAs**

Full-text PDF: <https://www.medscimonit.com/abstract/index/idArt/918382>

 3598

 1

 3

 41



Background

Worldwide, lung cancer remains the leading cause of mortality due to cancer, with high rates of recurrence and metastasis [1,2]. Non-small cell lung cancer (NSCLC) accounts for the majority (80%) of all cases of lung cancer, and adenocarcinoma is the most common subtype of NSCLC [3]. Surgical resection is the main first-line treatment for adenocarcinoma of the lung. In advanced NSCLC, patients are also treated with chemotherapy and targeted therapy, including epidermal growth factor receptor (EGFR) inhibitors [4], anaplastic lymphoma kinase (ALK) inhibitors [5], and immunotherapy, including immune checkpoint inhibitors [6,7]. Despite these recent clinical advances, the treatment of adenocarcinoma of the lung remains challenging due to tumor invasion, early metastasis, and drug resistance of tumor cells [8]. Therefore, continued studies are needed to identify the molecular basis of adenocarcinoma of the lung to develop new and more effective treatments.

Coatamer protein complex subunit beta 2 (COPB2) is a Golgi coatamer complex subunit, which is essential for Golgi vesicular trafficking and is essential during embryogenesis, particularly during the development of the brain [9]. Recent studies have shown that COPB2 is upregulated in several types of cancer and that knockdown of COPB2 might be a therapeutic target in human cancer [10,11]. A previously published study showed that silencing the COPB2 gene significantly inhibited the proliferation and invasion of A549 human lung cancer cells *in vitro* [12]. However, the functional role of COPB2 in adenocarcinoma of the lung remains unknown.

MicroRNAs (miRNAs) are small non-coding RNA molecules that bind to the 3'-untranslated region (3'UTR) of corresponding messenger RNAs (mRNAs). MiRNAs have been reported to have a potential role as diagnostic biomarkers in ovarian cancer [13], colorectal cancer [14], and pancreatic cancer [15]. In 2016, Zhou et al. identified a six-miRNA diagnostic panel that were upregulated in the plasma of patients with adenocarcinoma of the lung in an Asian population [16]. Also, for the treatment of human cancer, there is a potential role for miRNAs [17,18]. Cancer-associated miRNAs have been shown to act as oncogenes and tumor suppressors, and miRNAs that target the cell-cycle may be used to inhibit tumor growth [19]. In NSCLC, miRNAs may have potential roles in modulating metastases, either by inhibition or reconstitution of their functions [20]. In several human cancers, hsa-miR-335 has multiple roles in carcinogenesis [21–24]. Although little is known of the role of miR-335-3p in lung cancer, in several other cancers, miR-335-3p is down-regulated [25–28]. The expression of miR-335-3p in adenocarcinoma of the lung and the mechanism remain unknown, and there have been no previous studies on the miR-335-3p/COPB2 axis in adenocarcinoma of the lung or other cancers. Therefore, this study aimed to

investigate the role of microRNA (miRNA) targeting by COPB2 gene expression in human lung adenocarcinoma cell lines, including NCI-H1975 cells.

Material and Methods

Cell culture

Human BEAS-2B (CRL-9609) bronchial epithelial cells and human lung adenocarcinoma cell lines NCI-H1299 (CRL-5803), A549 (CCL-185), SK-MES-1 (HTB-58), NCI-H1688 (CCL-257) and NCI-H1975 (CRL-5908) were obtained from the American Tissue Culture Collection (ATCC) (Manassas, VA, USA). BEAS-2B cells were cultured in RPMI-1640 medium (61870044) (Gibco, Thermo Fisher Scientific, Waltham, MA, USA) supplemented with 10% heat-inactivated fetal bovine serum (FBS) (16140071) (Invitrogen, Carlsbad, CA, USA), l-glutamine 4 mM (25030081) (Gibco, Thermo Fisher Scientific, Waltham, MA, USA) and 1% penicillin-streptomycin, 100 U/ml and 100 µg/ml (5070063) (Gibco, Thermo Fisher Scientific, Waltham, MA, USA). NCI-H1299, A549, SK-MES-1, NCI-H1688 and NCI-H1975 cells were cultured in RPMI-1640 medium supplemented with 10% FBS and 1% penicillin-streptomycin. All cell lines were cultured in an incubator in a humidified atmosphere with 5% CO₂ at 37°C. Cells growing at an exponential phase were used for the subsequent experiments.

Cell transfection

A fluorescence-labeled transfection control short-interfering RNA (siRNA) (Control) (No. SR30002) (5'-AAAUCGUGAUUUGUGUAGUC-3') was used. The scrambled negative control siRNA (NC) (No. SR30004) (5'-CCUAAAGGUUAAGUCGCCUCG-3') and COPB2-siRNA (siCOPB2) (No. SR306142) were purchased from OriGene Technologies (Rockville, MD, USA). The miR-335-3p mimic (5'-UUUUUCAUUUUGCUCCUGACC-3') was purchased from GenePharma Co., Ltd. (Shanghai, China). The NCI-H1975 cells (4×10⁵ cells/well) were transfected with 110 pmol of siRNA or mimics in Opti-MEM reduced serum medium (11058021) (Invitrogen, Carlsbad, CA, USA) containing Lipofectamine 2000 (11668019) (Invitrogen, Carlsbad, CA, USA) at room temperature. After incubation for 24 h, cells were collected for subsequent functional analysis. The transfection efficiency after 48 h was detected by Western blot or quantitative reverse transcription-polymerase chain reaction (qRT-PCR).

The primer sequences for siCOPB2 included:

siCOPB2-1: 5'-CUCAUACGAAGAAUUGAAAUCAGC-3';
siCOPB2-2: 5'-UGCUUUGGACUAUGAGAAACUUCTT-3';
siCOPB2-3: 5'-GGAGCAGAAAGUAUCUACGGCGGCT-3'.

Table 1. Primers used for quantitative reverse transcription-polymerase chain reaction (qRT-PCR).

Gene	Forward	Reverse
COPB2 [32]	GTGGGGACAAGCCATACCTC	GTGCTCTCAAGCCGGTAGG
Cyclin D1	GCTGCGAAGTGGAACCATC	CCTCCTTCTGCACACATTGAA
TIMP-1	CTTCTGCAATTCGGACCTCGT	ACGCTGGTATAAGGTGGTCTG
MMP9	TGTACCGCTATGGTACACTCG	GGCAGGGACAGTTGCTTCT
Bcl-2	GGTGGGGTTCATGTGTGG	CGGTTCAAGTACTCAGTCATCC
Bax	CCCGAGAGGTCTTTTCCGAG	CCAGCCCATGATGGTTCTGAT
Hsa-miR-335-3p	TTTTTCATTATTGCTC	GTGCAGGGTCCGAGGT
GAPDH	GGAGCGAGATCCCTCCAAAT	GGCTGTTGCATACTTCTCATGG
U6	CTCGCTTCGGCAGCACA	AACGCTTCACGAATTTGCGT

RNA isolation and qualitative real-time polymerase chain reaction

Cells were treated with TRIzol reagent (15596026) (Invitrogen, Carlsbad, CA, USA) for 3–5 min on ice. After cell lysis, the total RNA was isolated and purified by using chloroform and isopropanol on ice. The concentration of RNA was measured by using NanoDrop 8000 (ND-8000-GL) (Thermo Fisher Scientific, Waltham, MA, USA). Then, 1 µg of RNA was reverse transcribed by using a PrimeScript II First Strand cDNA Synthesis Kit (6210B) (Takara, Tokyo, Japan). The mixture including RNA, the oligo dT primer, the PrimeScript RT Enzyme Mix I, and PrimeScript RT buffer, which was incubated at 37°C for 15 min, and 85°C for 5 s for reverse transcription. SYBR Green PCR Master Mix (4312704) (ABI Biosystems, Foster City, CA, USA) at 10 µl volumes, and Bio-Rad CFX 96 Touch Real-Time PCR Detection System (1855196) (Bio-Rad, Hercules, CA, USA) were used for the PCR reactions. The PCR parameters included denaturation at 95°C for 5 min, followed by denaturation at 95°C for 30 s, annealing at 60°C for 30 s, and extension at 72°C for 30 s. Glyceraldehyde-3-phosphate dehydrogenase (GAPDH) was used as an endogenous control. The $2^{-\Delta\Delta CT}$ method was used to calculate the relative expression levels. The qRT-PCR primers for cyclin D1, TIMP-1, MMP9, Bcl-2, and Bax were designed using Primerbank (<https://pga.mgh.harvard.edu/primerbank/>). The primers used for qRT-PCR are shown in Table 1.

To determine miRNA expression, total RNA, including miRNA, was isolated according to the above methods, using TaqMan MicroRNA Reverse Transcription Kit (4366597) (Applied Biosystems, Foster City, CA, USA). The miR-335-3p-specific primer used was: 5'-GTCGATCCAGTGCGTGTCTGGAGTCGGCAATGCACTGGATACGACGGTCAGGA-3'. The reaction mix including an RT primer pool of dNTPs with dTTP (100 mM), MultiScribe Reverse Transcriptase (50 U/µL), 10×RT buffer, RNase inhibitor, and 1 µg RNA, which were incubated at 16°C for 30 min, 42°C for 30 min, and 85°C for 5 min. The RT primer

pool included oligo dT, random primers, and the miR-335-3p-specific primer. The TaqMan miRNA Fluorescence Quantitative PCR Kit: Hsa-miR-335-3p and U6 snRNA were used for qRT-PCR (Thermo Fisher Scientific, Waltham, MA, USA). The Bio-Rad CFX 96 Touch Real-Time PCR Detection System was used for the reactions (Bio-Rad, Hercules, CA, USA). The PCR parameters included 95°C for 5 min, 40 cycles of 95°C for 15 s, 60°C for 30 s, and 70°C for 10 s. U6 snRNA was used as an endogenous control for data normalization. The comparative threshold cycle method $2^{-\Delta\Delta CT}$ was used to calculate the relative expression. The primers for qRT-PCR are shown in Table 1.

Western blot

Cells were gently washed three times in PBS and treated with pre-cooled cell lysis buffer containing 25 mM HEPES (7365-45-9) (Aladdin Reagents, Ltd., Shanghai, China), 2.5mM EDTA (E197262-1EA) (Aladdin Reagents, Ltd., Shanghai, China), 0.1% Triton X-100 (T109027) (Aladdin Reagents, Ltd., Shanghai, China), 1 mM of phenylmethyl sulfonyl fluoride (PMSF) (36978) (Thermo Fisher Scientific, Waltham, MA, USA) and 5 µg/ml of leupeptin (78435) (Thermo Fisher Scientific, Waltham, MA, USA). The protein was isolated by centrifuging the sample at 20,000×g at 4°C for 30 min. Total protein in the supernatants was collected and measured using a UV spectrophotometer (Beckman Coulter, Brea, CA, USA).

Proteins (50 µg) were separated on 4–20% sodium dodecyl sulfate-polyacrylamide gel electrophoresis (SDS-PAGE) gels and transferred to polyvinylidene fluoride (PVDF) membranes (LC2002) (Invitrogen, Carlsbad, CA, USA). The membranes were washed in TBST (50 mM Tris, 150 mM NaCl and 2% Tween-20, pH 7.5) three times at room temperature, blocked with 5% dried skimmed milk powder (PA201-01) (China BioMed, Shanghai, China) and incubated with primary antibodies at 4°C overnight. The primary antibodies were to COPB2 (PA5-77106) (1: 2000) (Thermo Fisher Scientific, Waltham, MA, USA), cyclin

D1 (ab134175) (1: 2000) (Abcam, Cambridge, UK), TIMP-1 (ab61224) (1: 2000) (Abcam, Cambridge, UK), MMP9 (ab73734) (1: 2000) (Abcam, Cambridge, UK), Bcl-2 (ab59348) (1: 2000) (Abcam, Cambridge, UK), Bax (ab32503) (1: 2000) (Abcam, Cambridge, UK). The membranes were incubated with the peroxidase-conjugated anti-rabbit secondary antibody (R3155) (1: 5000) (Sigma-Aldrich, St. Louis MO, USA) at 4°C overnight. The membranes were washed three times for 30 min in TBST and incubated in enhanced chemiluminescence (ECL) solution (Merck Millipore, Burlington, MA, USA) in the dark at room temperature for 1 min. The images were scanned and analyzed by using an ImageQuant ECL Imager (GE Healthcare Life Sciences, Logan, UT, USA). The samples were normalized to GAPDH.

Flow cytometry for assessment of cell-cycle arrest and apoptosis

The cell apoptosis rate of NCI-H1975 cells was evaluated by flow cytometry. NCI-H1975 cells at the logarithmic growth phase were selected and plated in a six-well plate at a density of 5×10^5 cells/well and incubated for 24 h at 37°C. The cells then underwent treatment. After treatment, the cells were washed three times in PBS and collected following centrifuging the sample at 1000 rpm at 4°C for 5 min.

The treated NCI-H1975 cells were incubated with 195 μ L of Annexin V- fluorescein isothiocyanate (FITC) mixture, and 5 μ L Annexin V- FITC (70-AP101-100-AVF) (MultiSciences Biotech Co. Ltd., Hangzhou City, China) were added to the suspended NCI-H1975 cells. After incubation at room temperature for 10 min in the dark, the cells were collected by centrifuging the sample, and the supernatant was discarded. Then, 195 μ L of the Annexin V-FITC mixture and 10 μ L of propidium iodide (PI) (BG-60910-00-200) (PeproTech, Rocky Hill, NJ, USA) were mixed and added to the cells on ice and in the dark. After mixing, the apoptosis rate was detected using a MoFlo Astrios Cell Sorter (B25982) (Beckman Coulter, Brea, CA, USA). The PI⁺/Annexin V⁺ double-positive cells were considered to be cells in apoptosis.

Transwell assays

The 6.5 mm transwells (3470) (Corning, New York, NY, USA) were used for the cell migration and invasion assays. In the migration assay, 5×10^4 cells per well were placed on the upper layer of the transwell, and a chemoattractant was on the lower layer of the Transwell. After culture at 37°C for 48 h, cells that traversed the well were fixed with methanol and stained with a 0.1% crystal violet solution. The migrated cell populations were evaluated in five random fields per well using a TS100 microscope (Nikon, Tokyo, Japan). In the cell invasion assay, cells were seeded into the transwell containing Matrigel, and a chemoattractant was on the lower layer of the

transwell. After culture at 37°C for 48 h, the cells that underwent cell invasion were fixed with methanol and stained with a 0.1% crystal violet solution. The invasive cell populations were evaluated in five random fields per well using a TS100 microscope (Nikon, Tokyo, Japan).

Cell Counting Kit-8 (CCK-8) assay

The Cell Counting Kit-8 (CCK-8) assay (70-CCK801) (MultiSciences Biotech Co. Ltd., Hangzhou City, China) was used to measure the proliferation of the NCI-H1975 cells. Briefly, the NCI-H1975 cells (3000 cells/well) were seeded in 96-well plates and cultured at 37°C for 24 h. CCK-8 solution (10 μ L) was added to each well. The NCI-H1975 cells were incubated at 37°C for 2.5 h. Cell viability was measured by measuring the absorbance at 450 nm.

Luciferase reporter assay

The bioinformatics website TargetScan 7.2 (www.targetscan.org) was used to identify COPB2 as the target gene of miR-335-3p. For the luciferase reporter assay, the cDNAs of wild-type COPB2-3'UTR (5'-TTTCCTTCTCAATAATGAAAT-3') and COPB2-3'UTR-mut (5'-TTTCCTTCTCAATATACTTTT-3') were synthesized by TsingKe Biotech Co., Ltd. (Beijing, China) and cloned into the luciferase reporter gene vector pmirGLO (E1330) (Promega, Madison, WI, USA) to construct the COPB2-3'-UTR plasmid and the COPB2-3'-UTR-mut plasmid. Firefly luciferase was used as the reporter for miRNA regulation of the 3'UTR. Briefly, the NCI-H1975 cells were maintained in 96-well plates and co-transfected with a luciferase reporter plasmid (0.05 μ g/well) and mimic (5 pmol). Cells were divided into four groups: cells transfected with control mimic and COPB2-3'UTR plasmid; cells transfected with miR-335-3p mimic COPB2-3'UTR plasmid; cells transfected with miR-335-3p mimic and COPB2-3'UTR-mut plasmid; and cells transfected with control mimic and COPB2-3'UTR-mut plasmid. After incubation at 37°C for 72 h, the firefly luciferase activity was measured by using the luciferase reporter assay system (N1610) (Promega, Madison, WI, USA) with a GloMax Discover System (GM3000) (Promega, Madison, WI, USA). The relative firefly reporter activity was calculated through normalization to the Renilla luciferase control.

Statistical analysis

Experiments were performed in triplicate. Data were presented as the mean \pm standard deviation (SD). GraphPad Prism version 6.0 (GraphPad Software, La Jolla, CA, USA) and SPSS version 18.0 (SPSS Inc, Chicago, IL, USA) were used for statistical analysis. Comparisons between quantitative variables performed using one-way analysis of variance (ANOVA) followed by Dunnett's post hoc test. A P-value <0.05 was considered to be statistically significant.

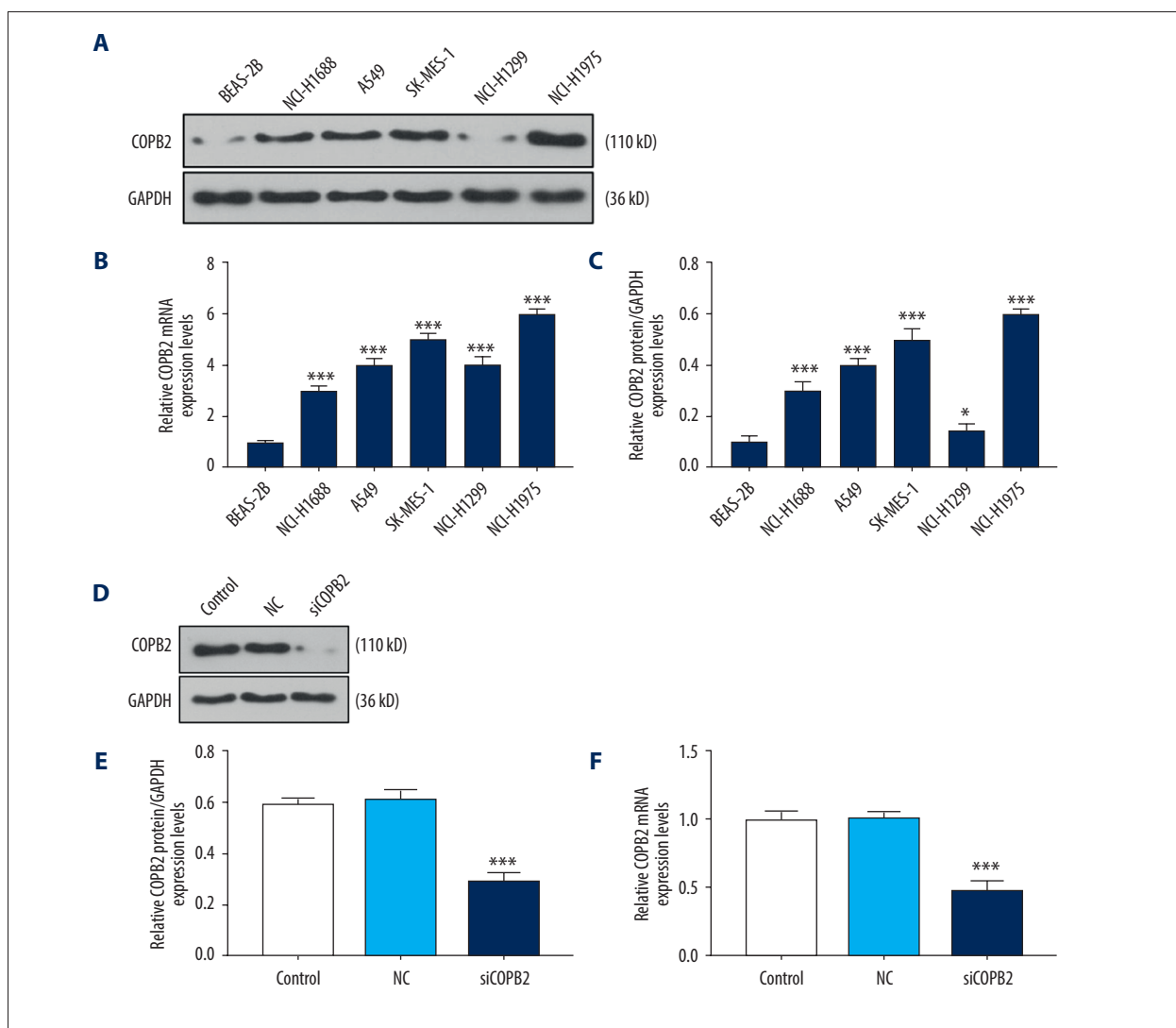
Results

The expression level and effects of COPB2 on cell apoptosis, invasion, migration, and proliferation of human lung adenocarcinoma cells

Western blot showed that the expression levels of COPB2 were significantly increased in human lung adenocarcinoma cells, NCI-H1688, A549, SK-MES-1, and NCI-H1975 ($P < 0.001$) and NCI-H1299 cells ($P < 0.05$) compared with BEAS-2B normal bronchial epithelial cells (Figure 1A, 1C). These findings were supported by quantitative reverse transcription-polymerase chain reaction (qRT-PCR) (Figure 1B). The expression level of COPB2 was greatest in NCI-H1975 cells (Figure 1A–1C). Therefore, NCI-H1975 cells were used in subsequent studies.

The fluorescence-labeled transfection control siRNA (Control), the scrambled negative control siRNA (NC), and short interfering

RNA (siRNA) resulting in knockdown of COPB2 (siCOPB2) were separately transferred into NCI-H1975 cells. The expression level of COPB2 was significantly down-regulated in NCI-H1975 cells after knockdown with siCOPB2 ($P < 0.001$) when measured by Western blot and qRT-PCR (Figures 1D–1F). The apoptosis rate of NCI-H1975 cells after knockdown with siCOPB2 was significantly increased when measured by flow cytometry ($P < 0.001$) (Figure 1G). The migration rate of NCI-H1975 cells after knockdown with siCOPB2 was significantly decreased when measured by transwell assays ($P < 0.001$) (Figure 1H). The invasion rate of NCI-H1975 cells after knockdown with siCOPB2 was significantly reduced when measured by transwell assays ($P < 0.001$) (Figure 1I). The proliferation rate of NCI-H1975 cells after knockdown with siCOPB2 at 24h, 48h, and 72h was significantly reduced when measured by the Cell Counting Kit-8 (CCK-8) assay (both, $P < 0.001$) (Figure 1J).



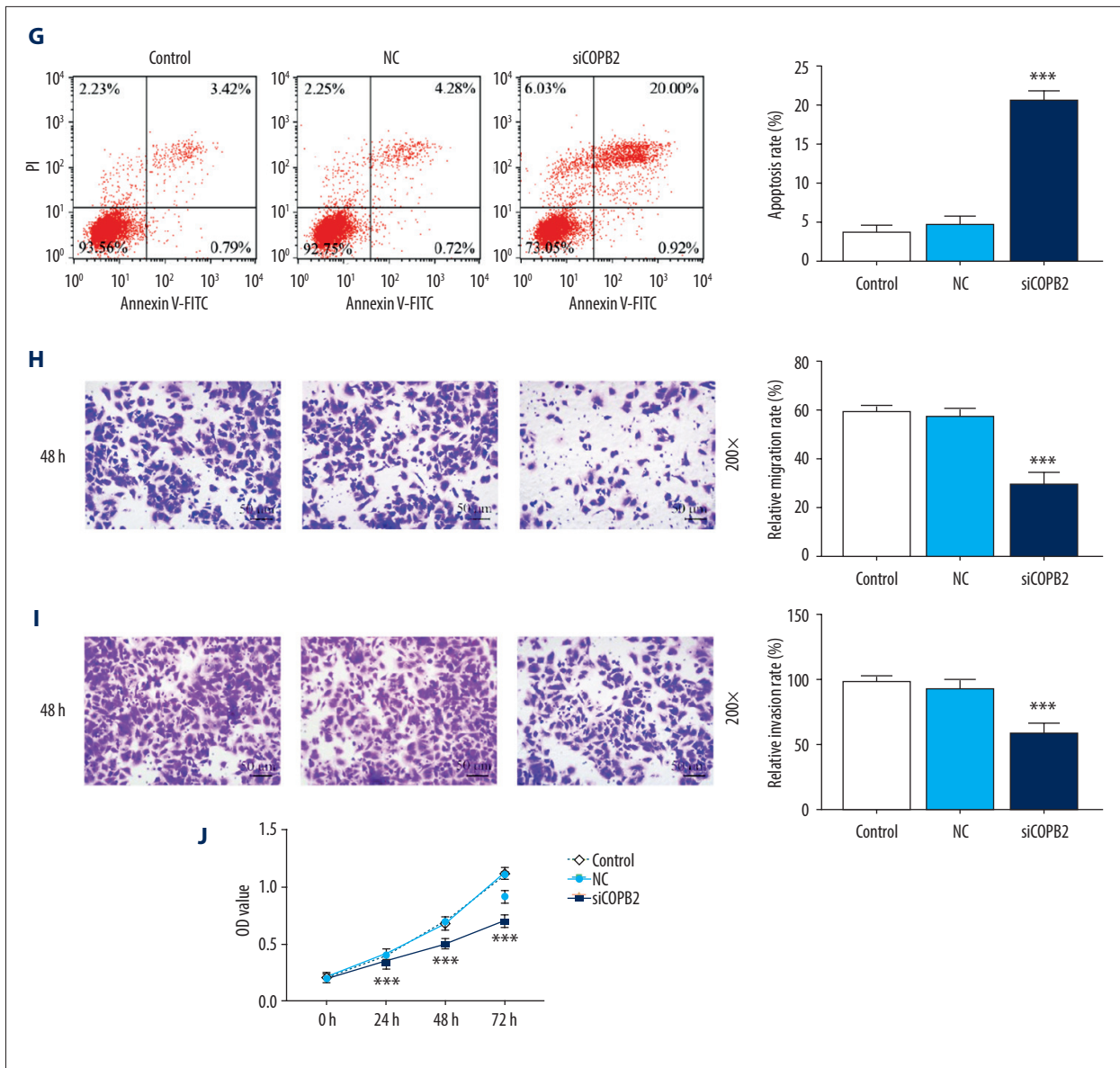


Figure 1. The expression levels of COPB2 in human adenocarcinoma cell lines and normal bronchial epithelial cells and the effects of knockdown COPB2 on cell proliferation, apoptosis, and migration in NCI-H1975 human adenocarcinoma cells. (A–C) Western blot and quantitative reverse transcription-polymerase chain reaction (qRT-PCR) show the expression level of COPB2 in BEAS-2B normal human bronchial epithelial cells and human lung adenocarcinoma cells, NCI-H1299, A549, SK-MES-1, NCI-H1688, and NCI-H1975. * $P < 0.05$, *** $P < 0.001$ vs. BEAS-2B. (D–F) Western blot and quantitative reverse transcription-polymerase chain reaction (qRT-PCR) show the relative expression level of COPB2 in NCI-H1975 cells. (G) The apoptosis rate of NCI-H1975 cells was measured by flow cytometry. The percentage of apoptotic cells, determined by propidium iodide (PI)⁺/Annexin V⁺, is shown in the right chart. (H) Photomicrograph of the transwell assay for NCI-H1975 cells. Magnification $\times 200$. The migration rate of NCI-H1975 cells is shown in the right chart. (I) Photomicrograph of the transwell assay for NCI-H1975 cells. Magnification $\times 200$. The invasion rate of NCI-H1975 cells is shown in the right chart. (J) Cell proliferation of NCI-H1975 cells detected by the Cell Counting Kit-8 (CCK-8) assay. *** $P < 0.001$ vs. NC. Control – fluorescence-labeled transfection control siRNA; NC – scrambled negative control siRNA; siCOPB2 – siRNA for knockdown of COPB2.

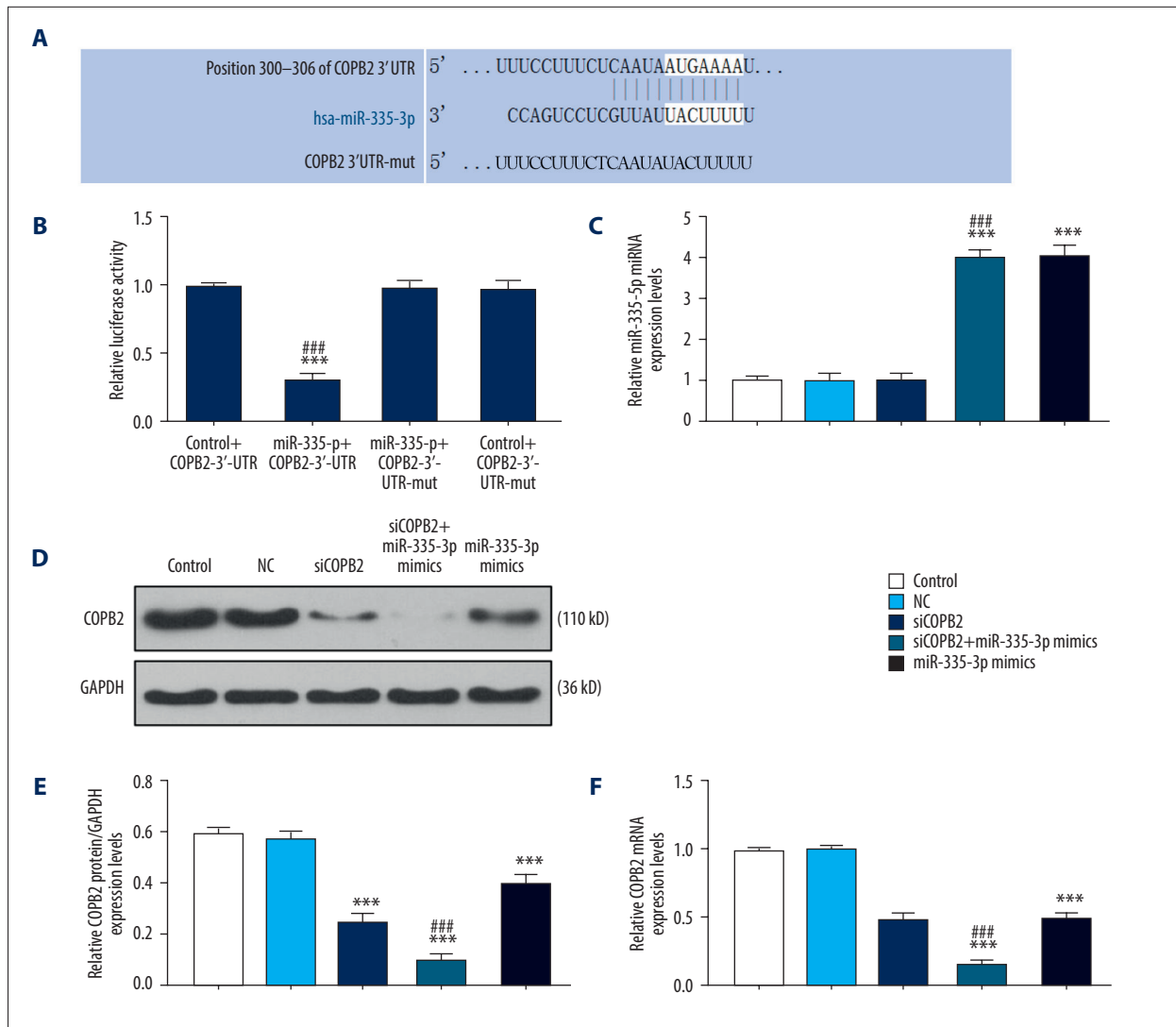
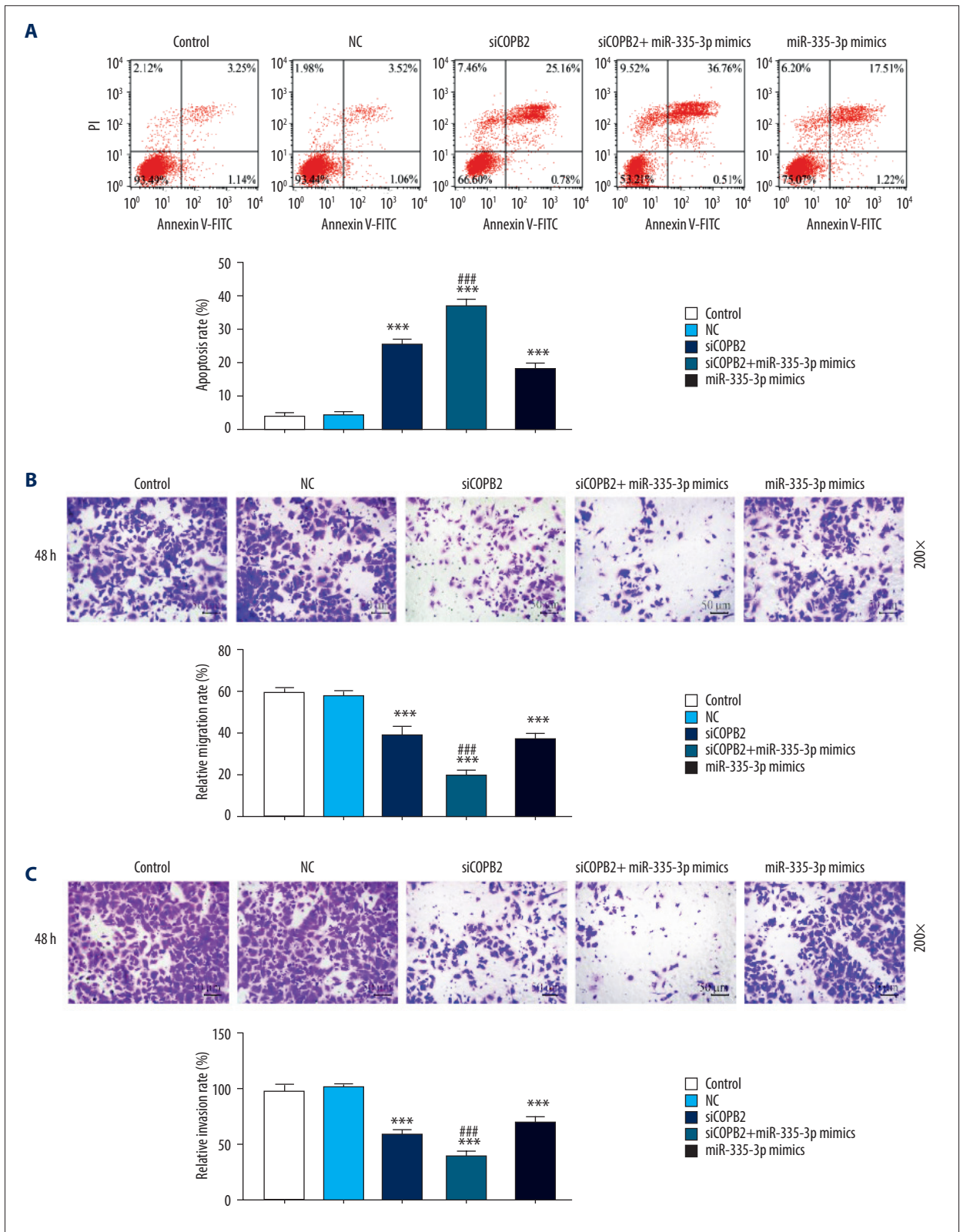


Figure 2. MicroRNA-335-3p (miR-335-3p) regulated the expression level of COPB2 by targeting 3'UTR of COPB2 mRNA in the NCI-H1975 human lung adenocarcinoma cells. **(A)** The potential target site for miR-335-3p in the 3'UTR of the COPB2 mRNA predicted by TargetScan 7.2. **(B)** Double-luciferase reporter assays were used to validate miR-335-3p binding of the COPB2 3'UTR in NCI-H1975 cells. *** $P < 0.001$ vs. Control+COPB2-3'-UTR. ### $P < 0.001$ vs. miR-335-3p+COPB2-3'-UTR-mut. **(C)** The relative miRNA expression level of miR-335-3p measured by quantitative reverse transcription-polymerase chain reaction (qRT-PCR) in NCI-H1975 cells. *** $P < 0.001$ vs. NC. ### $P < 0.001$ vs. siCOPB2. **(D–F)** Western blot and qRT-PCR analysis shows the expression level of COPB2 in NCI-H1975 cells. *** $P < 0.001$ vs. NC. ### $P < 0.001$ vs. siCOPB2. Control – fluorescence-labeled transfection control siRNA; NC – scrambled negative control siRNA; siCOPB2 – siRNA for knockdown of COPB2; siCOPB2+miR-335-3p mimics – co-transfection with siCOPB2 and miR-335-3p mimics.

MicroRNA-335-3p (miR-335-3p) regulated the expression level of COPB2 by targeting 3' UTR of COPB2 in NCI-H1975 human lung adenocarcinoma cells

A potential target site for miR-335-3p in the 3'UTR of the COPB2 mRNA was predicted by TargetScan 7.2 (Figure 2A). The double luciferase reporter assay showed that luciferase activity in NCI-H1975 cells co-transfected with miR-335-3p mimics and the COPB2 3'UTR vector were significantly reduced ($P < 0.001$), while luciferase activity in NCI-H1975 cells co-transfected with

miR-335-3p mimics and COPB2 3'UTR-mut was unchanged change ($P > 0.05$), compared with cells co-transfected with control and COPB2-3'UTR-mut (Figure 2B). Transfection with miR-335-3p mimics or si COPB2 in NCI-H1975 cells showed that miR-335-3p mimics, measured by qRT-PCR, showed significantly upregulated expression of miR-335-3p ($P < 0.001$). The knockdown of COPB2 had no effect on the expression of miR-335-3p ($P > 0.05$) (Figure 2C). Western blot and qRT-PCR analysis showed that siCOPB2 and miR-335-3p mimics both reduced the level of COPB2, and co-transfection with siCOPB2



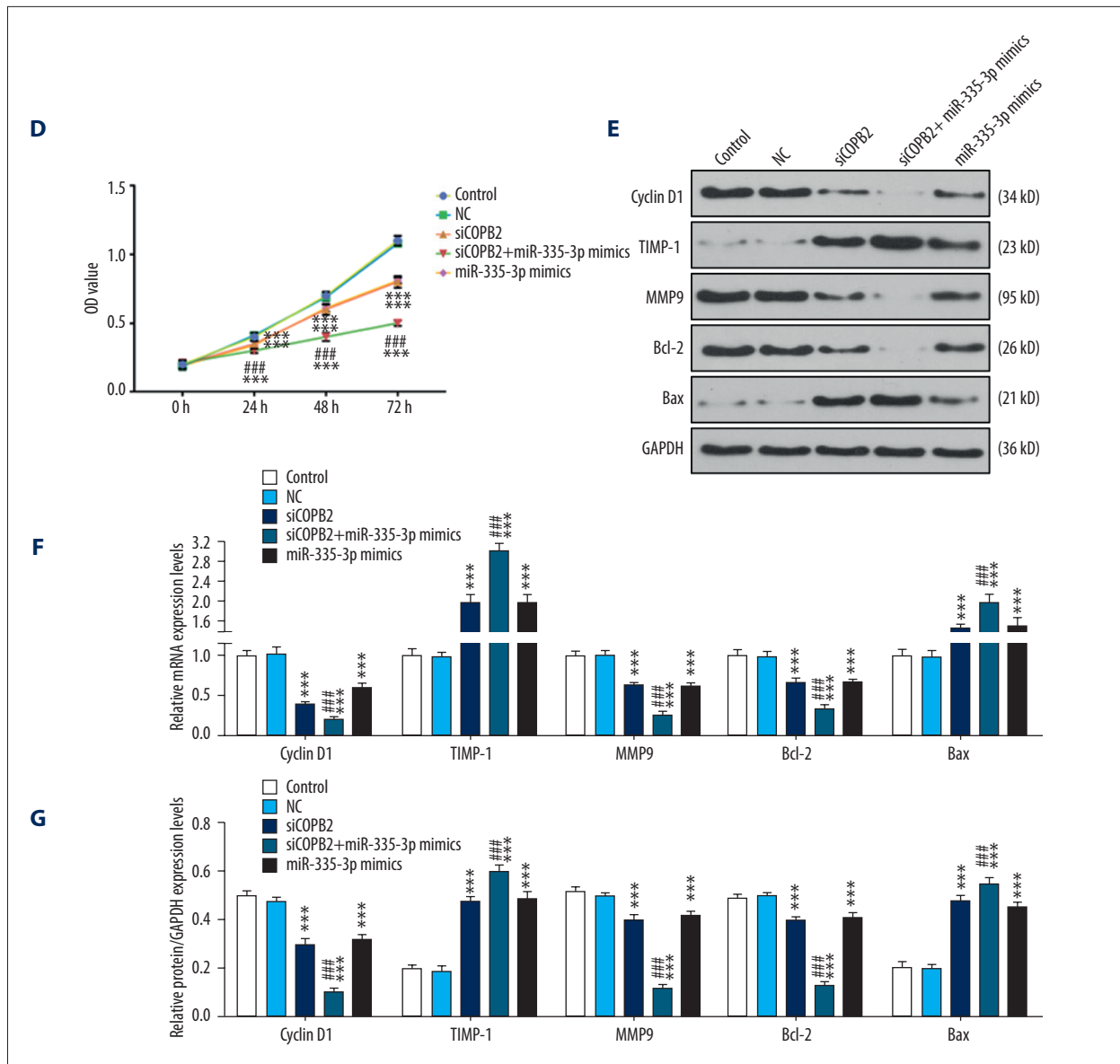


Figure 3. (A–G) MicroRNA-335-3p (miR-335-3p) regulated cell proliferation, apoptosis, and migration by targeting COPB2 mRNA in NCI-H1975 human lung adenocarcinoma cells. (A) The apoptosis rate of NCI-H1975 cells was measured by flow cytometry. The apoptosis rate is shown in the right chart. (B) Photomicrograph of the transwell assay for NCI-H1975 cells. Magnification $\times 200$. The migration rate of NCI-H1975 cells is shown in the right chart. (C) Photomicrograph of the transwell assay for NCI-H1975 cells. Magnification $\times 200$. The invasion rate of NCI-H1975 cells is shown in the right chart. (D) The proliferation capacity of NCI-H1975 cells measured by the Cell Counting Kit-8 (CCK-8) assay. (E) Western blot and quantitative reverse transcription-polymerase chain reaction (qRT-PCR) show the expression levels of cyclin D1, TIMP-1, MMP9, Bcl-2, and Bax in NCI-H1975 cells. *** $P < 0.001$ vs. NC. ### $P < 0.001$ vs. siCOPB2. Control – fluorescence-labeled transfection control siRNA; NC – scrambled negative control siRNA; siCOPB2 – siRNA for knockdown of COPB2; siCOPB2+miR-335-3p mimics – co-transfection with siCOPB2 and miR-335-3p mimics.

and miR-335-3p mimics significantly increased this effect (both $P < 0.001$) (Figure 2D–2F).

miR-335-3p regulated cell apoptosis, migration, and proliferation in NCI-H1975 human lung adenocarcinoma cells by targeting 3' UTR of COPB2

To investigate the effects of miR-335-3p on COPB2 in NCI-H1975 cells, the cell apoptosis rate and proliferation rate were evaluated by flow cytometry and CCK-8 assays, respectively. The migration and invasion rate of NCI-H1975 cells were determined by transwell assays. The apoptosis rate of NCI-H1975 cells after knockdown with siCOPB2 was significantly increased ($P < 0.001$), and miR-335-3p mimics significantly increased the effect of siCOPB2 ($P < 0.001$) (Figure 3A). The decrease in cell migration rate, cell invasion rate, and cell proliferation of NCI-H1975 cells following COPB2 knockdown was also significantly increased by miR-335-3p mimics (both $P < 0.001$) (Figure 3B–3D). The cell cycle proteins, cyclin D1, tissue inhibitor of metalloproteinases-1 (TIMP-1), and matrix metalloproteinase 9 (MMP9), and the cell apoptosis proteins, Bcl-2 and Bax, were measured by Western blot and qRT-PCR. Compared with cells transfected with siCOPB2 or miR-335-3p mimics, the expression levels of cyclin D1, MMP9, and Bcl-2 were highest in NCI-H1975 cells co-transfected with siCOPB2 and miR-335-3p mimics (both $P < 0.001$), and the expression of TIMP-1 and Bax were lowest in cells co-transfected with siCOPB2 and miR-335-3p mimics (both, $P < 0.001$) (Figure 3E–3G).

Discussion

Worldwide, non-small cell lung cancer (NSCLC), including adenocarcinoma of the lung, results in a major healthcare burden [10]. Adenocarcinoma of the lung can be highly invasive, and metastases can occur even with a small primary tumor, which means that many patients present with locally-advanced or metastatic disease, resulting in a low survival rate [29]. The aim of the present study was to investigate the role of microRNA (miRNA) targeting by the coatamer protein complex subunit beta 2 (COPB2) gene expression in human lung adenocarcinoma cell lines, including NCI-H1975 cells. The findings showed that COPB2 was an oncogene gene that regulated cell proliferation, apoptosis, migration and invasion of NCI-H1975 cells *in vitro*. Also, microRNA-335-3p (miR-335-3p) inhibited the function of COPB2 by targeting 3'UTR of COPB2 in NCI-H1975 cells. These findings identified the miR-335-3p/COPB2 axis in human lung adenocarcinoma cells, and indicate that further studies are required to determine whether the miR-335-3p/COPB2 axis has potential diagnostic or therapeutic roles in adenocarcinoma of the lung.

COPB2 is upregulated in several cancers, and functional studies have shown that COPB2 is down-regulated in cervical cancer cells [30]. The expression pattern and function of COPB2 in appears to differ in different types of cancer. In the present study, COPB2 was overexpressed in NCI-H1975 human lung adenocarcinoma cells, and silencing COPB2 resulted in increased cell apoptosis, and reduced cell proliferation, cell invasion, and cell migration *in vitro*. These findings are supported by those from a previous study that showed that knockdown of COPB2 inhibited the cell cycle pathway, inducing G₀/G₁ and S-phase cell cycle arrest in colon cancer cells [30]. Previous studies in adenocarcinoma of the lung have shown that COPB2 regulates cell apoptosis and promotes cell proliferation by regulating YAP1 expression [31]. These findings support that COPB2 may have a role in the progression of some types of human malignancy.

However, the mechanisms for the effects of COPB2 in human cancer cells remain unknown. Several previous studies have shown that dysfunction of microRNAs has a key role in tumorigenesis [31] and metastasis [32]. In the cytoplasm, RNA-induced silencing complex (RISC) contains members of the Argonaute (AGO) gene family, siRNAs, miRNAs, or siRNA-complementary mRNAs. MiRNAs in RISC bind to the 3'-UTR or untranslated region of target mRNA, inhibiting the corresponding gene expression. Considering the characteristics of miRNAs, this study aimed to investigate miRNA targeting of COPB2, and showed that COPB2 was a functional target gene for miR-335-3p.

In previous studies, miR-335-3p is down-regulated white adipose tissue [33], and also regulates sodium transport in the kidney [34]. Some studies have shown that miR-335-3p has a tumor suppressor role in gastric and pancreatic cancers [27,28]. In the present study, miR-335-3p directly bound with the 3'-UTR of COPB2. By transfection with miR-335-3p mimics or co-transfection with siCOPB2 and miR-335-3p mimics, miR-335-3p inhibited the expression level of COPB2. A previous study showed that miR-335-5p and miR-335-3p inhibited estrogen receptor alpha (ER α) expression in breast cancer cells [35]. Also, miR-335-3p is involved in Epstein-Barr virus (EBV)-associated gastric cancer, and is down-regulated in gastric cancer through the β -catenin signaling pathway [36]. However, the function of miR-335-3p and its related molecular mechanisms in cancer remain unclear. In the present study, COPB2 was shown to be a functional target of miR-335-3p in NCI-H1975 human adenocarcinoma cells.

Also, the findings in this study showed that overexpression of miR-335-3p increased cell apoptosis and inhibited cell proliferation, invasion, and migration in lung adenocarcinoma cells by targeting COPB2. The levels of cyclin D1, TIMP-1, MMP9, Bcl-2, and Bax were measured by quantitative reverse transcription-polymerase chain reaction (qRT-PCR) and Western blot and showed the effects of miR-335-3p on lung

adenocarcinoma cells through COPB2. Cyclin D1 is a regulatory subunit of CDK4 or CDK6, and plays an important role in cell cycle G1/S transition. TIMP-1 is a secreted protein and inhibits MMPs, changing extracellular matrix (ECM) and reduces cell motility [37]. The expression of MMP9 in adenocarcinoma of the lung is positively associated with a metastatic phenotype [38], and has also been used to assess the invasive capacity of cancer cells [39]. Bcl-2 is a cell apoptosis inhibitor, which has the function of preventing cell apoptosis [40]. Bax is a cell apoptosis regulator and antagonizes the function of Bcl-2 by forming a heterodimer with Bcl-2 [41]. The findings from the present study showed that miR-335-3p mimics promoted the down-regulation of cyclin D1, MMP9, Bcl-2, and the increase of TIMP-1 and Bax caused by COPB2 knockdown in NCI-H1975 cells. However, the findings from the present *in vitro* study in NCI-H1975 requires confirmation in other lung adenocarcinoma cell lines, and functional *in vivo* studies.

References:

1. Siegel RL, Miller KD, Jemal A: Cancer statistics, 2018. *Cancer J Clin*, 2018; 68(1): 7–30
2. Bray F, Ferlay J, Soerjomataram I et al: Global cancer statistics 2018: GLOBOCAN estimates of incidence and mortality worldwide for 36 cancers in 185 countries. *Cancer J Clin*, 2018; 68(6): 394–424
3. Wang D, Chen TY, Liu FJ: Che-1 attenuates hypoxia/reoxygenation-induced cardiomyocyte apoptosis by upregulation of Nrf2 signaling. *Eur Rev Med Pharmacol Sci*, 2018; 22(4): 1084–93
4. Murtuza A, Bulbul A, Shen JP et al: Novel third-generation EGFR tyrosine kinase inhibitors and strategies to overcome therapeutic resistance in lung cancer. *Cancer Res*, 2019; 79(4): 689–98
5. Aubry A, Galiacy S, Allouche M: Targeting ALK in cancer: Therapeutic potential of proapoptotic peptides. *Cancers (Basel)*, 2019; 11(3): pii: E275
6. Hendriks LEL, Henon C, Auclin E et al: Outcome of non-small cell lung cancer patients with brain metastases treated with checkpoint inhibitors. *J Thorac Oncol*, 2019; 14(7): 1244–54
7. Saad MI, Alhayani S, McLeod L et al: ADAM17 selectively activates the IL-6 trans-signaling/ERK MAPK axis in KRAS-addicted lung cancer. *EMBO Mol Med*, 2019; 11(4): pii: e9976
8. Politi K, Herbst RS: Lung cancer in the era of precision medicine. *Clin Cancer Res*, 2015; 21(10): 2213–20
9. DiStasio A, Driver A, Sund K et al: Copb2 is essential for embryogenesis and hypomorphic mutations cause human microcephaly. *Hum Mol Genet*, 2017; 26(24): 4836–48
10. Cheng T-YD, Cramb SM, Baade PD et al: The international epidemiology of lung cancer: Latest trends, disparities, and tumor characteristics. *J Thorac Oncol*, 2016; 11(10): 1653–71
11. Li ZS, Liu CH, Liu Z et al: Downregulation of COPB2 by RNAi inhibits growth of human cholangiocellular carcinoma cells. *Eur Rev Med Pharmacol Sci*, 2018; 22(4): 985–92
12. Erdogan E, Klee EW, Thompson EA, Fields AP: Meta-analysis of oncogenic protein kinase Ciota signaling in lung adenocarcinoma. *Clin Cancer Res*, 2009; 15(5): 1527–33
13. Wee Y, Liu Y, Lu J et al: Identification of novel prognosis-related genes associated with cancer using integrative network analysis. *Sci Rep*, 2018; 8(1): 3233
14. Moreno EC, Pascual A, Prieto-Cuadra D et al: Novel molecular characterization of colorectal primary tumors based on miRNAs. *Cancers (Basel)*, 2019; 11(3): pii: E346
15. Zhang Z, Qin H, Jiang B et al: miR-30e-5p suppresses cell proliferation and migration in bladder cancer through regulating metadherin. *J Cell Biochem*, 2019; 120(9): 15924–32
16. Zhou X, Wen W, Shan X et al: A six-microRNA panel in plasma was identified as a potential biomarker for lung adenocarcinoma diagnosis. *Oncotarget*, 2016; 8(4): 6513–25
17. Mao Z, Li H, Du B et al: LncRNA DANCR promotes migration and invasion through suppression of lncRNA-LET in gastric cancer cells. *Biosci Rep*, 2017; 37(6): pii: BSR20171070
18. Zhao Z, Li L, Du P et al: Transcriptional downregulation of miR-4306 serves as a new therapeutic target for triple negative breast cancer. *Theranostics*, 2019; 9(5): 1401–16
19. Hydrbring P, Wang Y, Bogorad RL et al: Cell-cycle-targeting microRNAs as therapeutic tools against refractory cancers. *Cell Cycle*, 2017; 16(23): 2241–48
20. Weidle UH, Birzele F, Nopora A: MicroRNAs as potential targets for therapeutic intervention with metastasis of non-small cell lung cancer. *Cancer Genomics Proteomics*, 2019; 16(2): 99–119
21. Sandoval-Bórquez A, Polakovicova I, Carrasco-Véliz N et al: MicroRNA-335-5p is a potential suppressor of metastasis and invasion in gastric cancer. *Clin Epigenetics*, 2017; 9: 114
22. Wang K, Chen X, Zhan Y et al: miR-335 inhibits the proliferation and invasion of clear cell renal cell carcinoma cells through direct suppression of BCL-W. *Tumor Biol*, 2015; 36(9): 6875–82
23. Liu J, Bian T, Feng J et al: miR-335 inhibited cell proliferation of lung cancer cells by target Tra2β. *Cancer Sci*, 2018; 109(2): 289–96
24. Luo LJ, Wang DD, Wang J et al: Diverse roles of miR-335 in development and progression of cancers. *Tumor Biol*, 2016; 37(12): 15399–410
25. Martin EC, Conger AK, Yan TJ et al: MicroRNA-335-5p and -3p synergize to inhibit estrogen receptor alpha expression and promote tamoxifen resistance. *FEBS Lett*, 2017; 591(2): 382–92
26. Roberto GM, Delsin LEA, Vieira GM et al: ROCK1-predicted microRNAs dysregulation contributes to tumor progression in ewing sarcoma. *Pathol Oncol Res*, 2017 [Epub ahead of print]
27. Kaur S, Krishn SR, Rachagani S, Batra SK: Significance of microRNA-based biomarkers for pancreatic cancer. *Ann Transl Med*, 2015; 3(18): 277
28. Jing JJ, Wang ZY, Li H et al: Key elements involved in Epstein-Barr virus-associated gastric cancer and their network regulation. *Cancer Cell Int*, 2018; 18: 146
29. Siegel RL, Miller KD, Jemal A: Cancer statistics, 2019. *Cancer J Clin*, 2019; 69(1): 7–34
30. Tan MS, Chang SW, Cheah PL, Yap HJ: Integrative machine learning analysis of multiple gene expression profiles in cervical cancer. *Peer J*, 2018; 6: e5285
31. Pu X, Wang J, Li W et al: COPB2 promotes cell proliferation and tumorigenesis through upregulating YAP1 expression in lung adenocarcinoma cells. *Biomed Pharmacother*, 2018; 103: 373–80

Conclusions

This study aimed to investigate the role of microRNA (miRNA) targeting by COPB2 gene expression in human lung adenocarcinoma cell lines. The findings showed that COPB2 was the functional target of microRNA-335-3p (miR-335-3p) in NCI-H1975 human adenocarcinoma cells. The findings indicated that COPB2 might be an oncogene in lung adenocarcinoma cells by functioning as a target of miR-335-3p. These preliminary *in vitro* findings from a study in a single human lung adenocarcinoma cell line require study in other cell lines and support from further functional studies.

Conflict of interest

None.

32. Wu SG, Chang TH, Liu YN, Shih JY: MicroRNA in lung cancer metastasis. *Cancers (Basel)*, 2019; 11(2): pii: E265
33. Oger F, Gheeraert C, Mogilenko D et al: Cell-specific dysregulation of microRNA expression in obese white adipose tissue. *J Clin Endocrinol Metab*, 2014; 99(8): 2821–33
34. Edinger RS, Coronello C, Bodnar AJ et al: Aldosterone regulates microRNAs in the cortical collecting duct to alter sodium transport. *J Am Soc Nephrol*, 2014; 25(11): 2445–57
35. Martin EC, Conger AK, Yan TJ et al: MicroRNA-335-5p and -3p synergize to inhibit estrogen receptor alpha expression and promote tamoxifen resistance. *FEBS Lett*, 2017; 591(2): 382–92
36. Dong L, Deng J, Sun ZM et al: Interference with the beta-catenin gene in gastric cancer induces changes to the miRNA expression profile. *Tumour Biol*, 2015; 36(9): 6973–83
37. Tsai CH, Cheng HC, Wang YS et al: Small GTPase Rab37 targets tissue inhibitor of metalloproteinase 1 for exocytosis and thus suppresses tumour metastasis. *Nat Commun*, 2014; 5: 4804
38. Cai X, Zhu H, Li Y: PKC ζ , MMP-2 and MMP-9 expression in lung adenocarcinoma and association with a metastatic phenotype. *Mol Med Rep*, 2017; 16(6): 8301–6
39. Tsoyi K, Osorio JC, Chu SG et al: Lung adenocarcinoma Syndecan-2 potentiates cell invasiveness. *Am J Respir Cell Mol Biol*, 2019; 60(6): 659–66
40. Delbridge AR, Grabow S, Strasser A, Vaux DL: Thirty years of BCL-2: Translating cell death discoveries into novel cancer therapies. *Nat Rev Cancer*, 2016; 16(2): 99–109
41. Chen HC, Kanai M, Inoue-Yamauchi A et al: An interconnected hierarchical model of cell death regulation by the BCL-2 family. *Nat Cell Biol*, 2015; 17(10): 1270–81